N87-20278

EXPERIMENTAL INVESTIGATION OF PILOTED FLAMEHOLDERS

C.F. Guo, Y.H. Zhang, and Q.M. Xie
Gas Turbine Research Institute
Jiangyou County of Sichuan, People's Republic of China

Four configurations of piloted flameholders were tested. The range of flame stabilization, flame propagation, pressure oscillation during ignition, and pressure drop of the configurations were determined. Some tests showed a very strong effect of inlet flow velocity profile and flameholder geometry on flame stabilization.

INTRODUCTION

Pressure oscillation during the transient period from ignition to maximum augmentation is a critical problem for the turbofan augmentor. Since this pressure oscillation may cause fan flow to stall or surge, it is important to know the peak pressure during augmentor ignition and to take some kind of technical measure to reduce this peak pressure. Such a procedure is called "soft ignition."

The combustion process in the fan flow of a turbofan augmentor is under a severe condition. It is helpful to understand how to make use of the hot combustion products in the core stream to ignite the combustible mixture in the cold fan stream. The present research compares the capability for soft ignition and the ability of different configurations of piloted flameholders to ignite a cold fan stream.

SYMBOLS

C pressure loss coefficient

F area

G_a air-mass flow rate

G_f fuel flow rate

h gap height of V-gutter or peripheral length of test section

M Mach number

P pressure, kg/cm^2

P* stagnant pressure, kg/cm^3

ΔP pressure drop or pressure oscillation value, kg/cm^2

T temperature, °C

T* stagnant temperature, °C

V velocity, m/sec

AFR air-fuel ratio

Subscripts:

0 upstream of flow orifice

1 downstream of flow orifice or upstream of air heater

2 inlet of test section

3 outlet of test section

a air or ambient

ave average

APPARATUS

The test apparatus is shown in figure 1. The airflow from the compressor is divided into two streams: one stream goes to ejector 7 to create a low-pressure exhaust condition for the test section; the other stream goes through valve 1, flow-orifice meter 2, air heater 3, control valve 4, and plenum chamber 5 into test section 6. After leaving the test section the combustion products are cooled by water injection. The hot gas is exhausted into the ambient through the ejector.

The test rig assembly is shown in figure 2. It is a rectangular duct 300 mm by 175 mm. The piloted flameholder is mounted inside the test section by bolts. Flame extinction is recorded through a quartz window by a flame-detection device. Flame extinction can also be observed visually. The ignition in the primary zone is provided by a high-energy ignitor of 12 J. The combustible mixture in the secondary zone is ignited by flame propagation from the primary zone. The inlet flow is measured by the static pressure tap, the stagnant pressure tube, and the chromel-alumel thermocouple. The outlet temperature is monitored by a platinum/platinum-rhodium thermocouple. Outlet stagnant pressure is measured by three water-cooled stagnant pressure probes; each has three measuring points. The transient pressure is measured by an induction-type pressure transducer (CYG-1, 0 to 1.0 kg/cm^2) with an LR-1 carrier wave amplifier and an Sc-60 ultraviolet oscilloscope. The fuel flow rate is measured by a turbine-type flowmeter with a digital frequency indicator.

The fuel is injected through a spray bar. There is one spray bar in the primary zone. The total length of the bar is 280 mm. There are six pairs of holes (0.4 mm in diam) on the bar at an intersection angle of 60°. In the secondary zone there are six spray bars. The two bars in the center have four pairs of holes (0.35 mm in diam) at an intersection angle of 30°; the other four spray bars have four holes (0.35 mm in diam) each. Fuel injection in the secondary zone is in the counterflow direction. The test configurations of piloted flameholders are shown in figure 3.

TEST METHOD

The test conditions were as follows:

T_2^* 60 to 70 °C or 500 °C

M_2 0.23

P_2^* 0.25 to 1.2 kg/cm^2

The test procedures were as follows: First, the air supply was adjusted to maintain the inlet conditions of P_2^*, M_2, and T_2^* as specified. After the primary zone had been ignited the ejector air supply was adjusted to maintain P_2^*, M_2, and T_2^* constant. Then the fuel flow in the primary zone G_{fp} was increased until fuel-rich flameout occurred. After that, the primary zone was reignited at the specified inlet condition and P_2^*, M_2, and T_2^* were kept constant. Finally, the fuel flow was reduced until there was fuel-lean flame extinction. Before ignition, the pressure drop between the inlet and outlet was measured. During ignition the peak pressure, the fuel-air mixture in the secondary zone, and the pressure oscillation were also recorded.

RESULTS AND DISCUSSION

Peak Pressure Measurements

As shown in figure 4, the peak pressure rise during ignition is usually lower than 10 percent of the inlet pressure ($\Delta P_2/P_2^* < 10$ percent). The peak pressure rise in the augmentor is normally related to the amount of fuel injected (as in these tests). Since the ignition is realized in a small volume, the amount of fuel necessary for ignition is small. Thus, the peak pressure is lower than that for normal augmentor ignition. This proves that using a piloted flameholder makes it easier to obtain a soft ignition in a turbofan augmentor.

Pressure Oscillation Measurements

Pressure oscillation measurements were performed under the same conditions as the peak pressure measurements. The amount of fuel injected in the primary zone has a very strong effect on the pressure oscillation in the augmentor during ignition in the secondary zone (figs. 5(a) and (b)). It has been shown that, with the same amount of fuel injected in the secondary zone, the pressure oscillation during the onset of secondary combustion varies with the amount of fuel injected in the primary zone. It is clear that there is an optimum fuel injection in the primary zone which minimizes the pressure oscillation during secondary zone ignition.

Flow Resistance

Figure 6 shows the variation of the pressure loss coefficient with the Reynolds number Re for different configurations. When Re increases, the pressure loss coefficient C decreases slightly. The pressure loss coefficient C also decreases with the increase of gap height h. The pressure loss coefficient C for a V-gutter is slightly lower than that for a semispherical shape.

Effect of Inlet Flow Distortion

The inlet flow distortion is shown in figure 7. Figure 8 shows the effect of inlet flow distortion on flame stabilization. When the inlet flow is distorted, the range of flame stabilization is narrowed, and the peak value of the stabilization parameter is also reduced. For instance, at $P_2^* = 0.25$ kg/cm^2 when there is no inlet distortion, it is possible to ignite the secondary zone in 3 sec; but, when there is inlet distortion (even at $P_2^* = 0.3$ kg/cm^2), the range of flame stabilization is very narrow and the ignitability in the secondary zone is very weak. (It is impossible to ignite the fuel-air mixture in the secondary zone.)

Effect of Secondary Air Entry Holes on Stabilization of the SJ410-4A Flameholder

When 54 secondary holes (8 mm in diam) are opened, the range of flame stabilization is very narrow (fig. 9). When these holes are blocked, the stabilization range is broader. The secondary air entry holes also reduce the capability of igniting the fuel-air mixture in the secondary zone. It seems that the secondary air dilutes the primary combustion products and reduces the temperature.

Effect of Gap Height

Figure 10(a) and (b) show the effect of gap height h on flame stabilization for the SJ410-4B and SJ410-3A configurations. The range of flame stabilization decreases with the increase of the gap height h, and the ignitability also decreases. From this test we found that, for a specified configuration, there is an optimum gap height. For instance, when the width of the V-gutter is 70 mm (SJ410-3A), the optimum gap height is 3 to 5 mm, the width of V-gutter is 40 mm (SJ410-4B), and the optimum gap height is 2 to 3 mm. Under these conditions, the range of ignition and flame stabilization and the ignition capability in the secondary zone are nearly the same for the two configurations.

Effect of Bluff Body Shape on Flame Stabilization

Figure 11(a) shows the flame stabilization range for the SJ410-3A configuration under ambient air temperature with a different bluff body shape. The range of flame stabilization of the V-gutter bluff body is wider than that of the semispherical bluff body. But as shown in figure 11(b), at $T_2^* = 500$ °C the ranges of flame stabilization for both bluff bodies are nearly the same. This can be explained as follows. At high inlet temperature, the vaporization rate of the fuel spray (before entering the primary zone) is high for both flameholders; therefore, the gaseous fuel-air ratios of the mixtures in the primary zone are nearly the same. But at low temperature, the fuel vaporization rate on the V-gutter surface is higher than that on the semi-spherical body, and the fuel-air ratio in the primary zone of the V-gutter is higher than that of the semi-spherical body. Thus, the V-gutter has a wider range of flame stabilization.

Effect of Air Entry Holes in V-Gutter Wall on Flame Stabilization

Figure 12 shows the range of flame stabilization for the SJ410-3B configuration with different air entry holes in the V-gutter wall. For a given

opening area, fewer holes with larger diameters offer better flame stabilization than smaller holes. A comparison of figure 10(b) with figure 12 shows that the recirculation zone created by the gap provides better flame stabilization than that created by circular holes.

CONCLUSIONS

These tests led to the following conclusions.

(1) The use of a piloted flameholder in the turbofan augmentor may minimize the peak pressure rise during ignition. At the present experimental conditions, $\Delta P/P_2^*$ is less than 10 percent; therefore, the use of a piloted flameholder is a good method to realize soft ignition.

(2) The geometry of the piloted flameholder and the amount of fuel injected into the flameholder have a strong effect on the pressure oscillation during ignition of the fuel-air mixture in the secondary zone.

(3) Compared with the V-gutter flameholder with holes in its wall, the V-gutter flameholder without holes not only has the advantages such as simple structure and good rigidity but offers a wide combustion stability limit and a high capability of igniting the fuel-air mixture of the secondary zone.

BIBLIOGRAPHY

Branstetter, J.R.; and Juhasz, A.J.: Experimental Performance and Combustion Stability of a Full Scale Duct Burner for a Supersonic Turbofan Engine. NASA TN D-6163, 1971.

Cullom, R.R.; and Johnsen, R.L.: Operating Condition and Geometry Effects on Low-Frequency Afterburner Combustion Instability in a Turbofan at Altitude. NASA TP-1475, 1979.

Kurkov, A.P.: Turbofan Compressor Dynamics During Afterburner Transients. NASA TM X-71741, 1975.

Marshall, R.L.; and Canuel, G.E.: Augmentation Systems for Turbofan Engines. Presented at Crafield International Symposium, 1976.

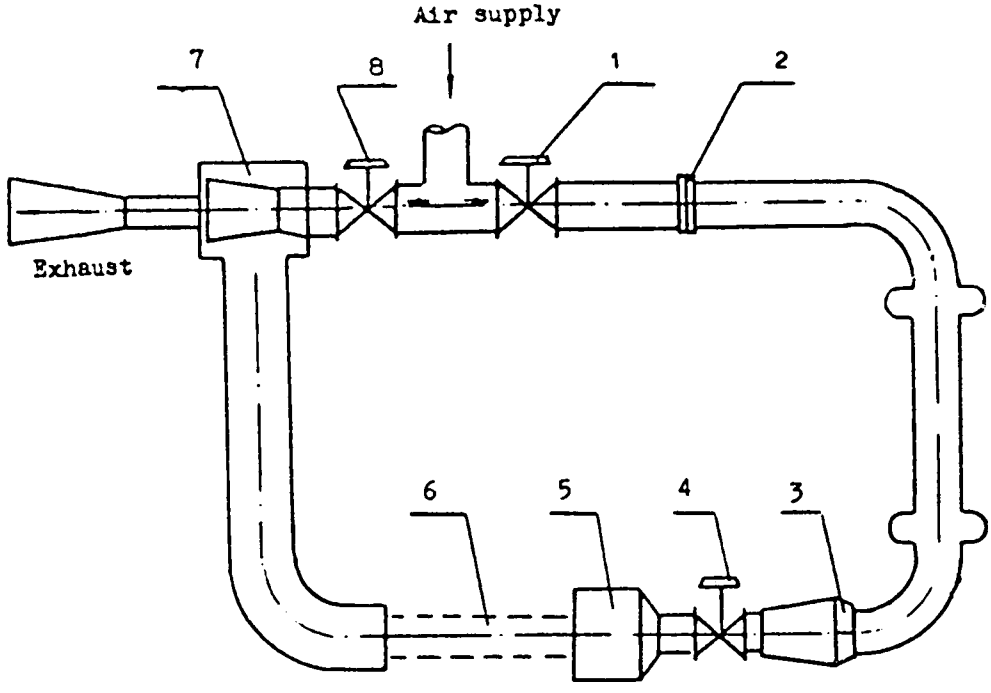

Figure 1. - Test apparatus. Valve, 1; orifice flowmeter, 2; air heater, 3; control valve, 4; plenum chamber, 5; test section, 6; ejector, 7; valve, 8.

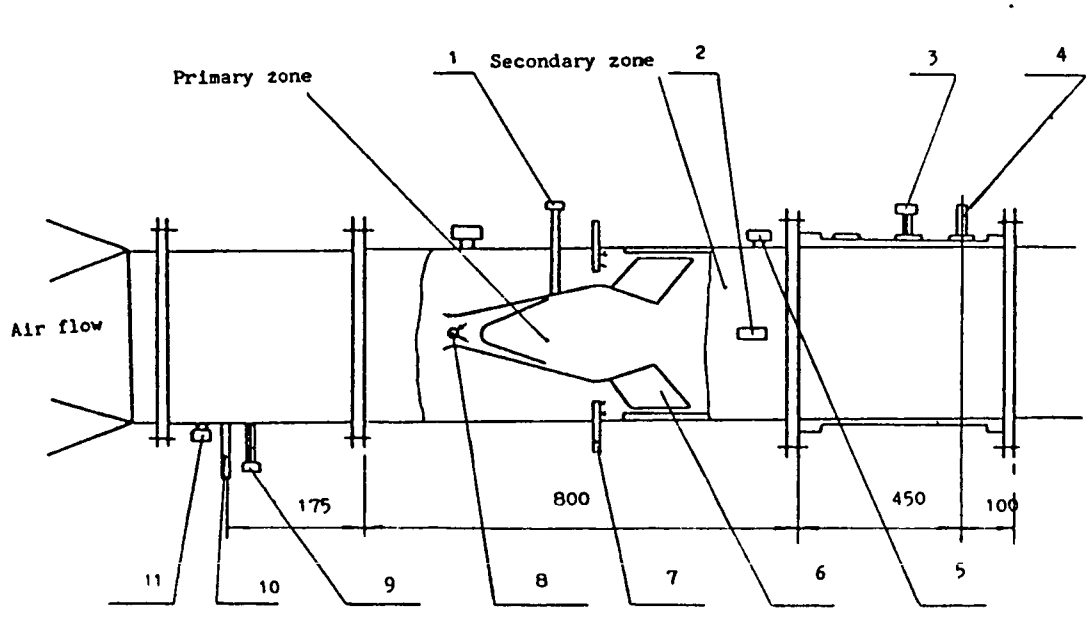

Figure 2. - Test rig assembly. High energy ignitor, 1; quartz window, 2; thermocouple, 3; pressure probe, 4; pressure transducer, 5; test configuration, 6; fuel spray, 7; fuel spray bar, 8; thermocouple, 9; pressure probe, 10; pressure tap, 11.

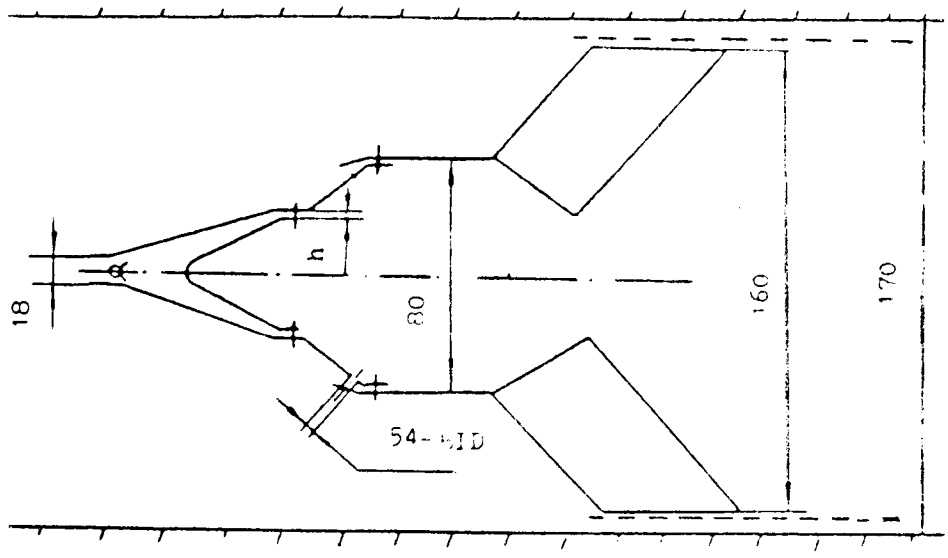

(a) Configuration SJ410-4A; h = 4 mm.

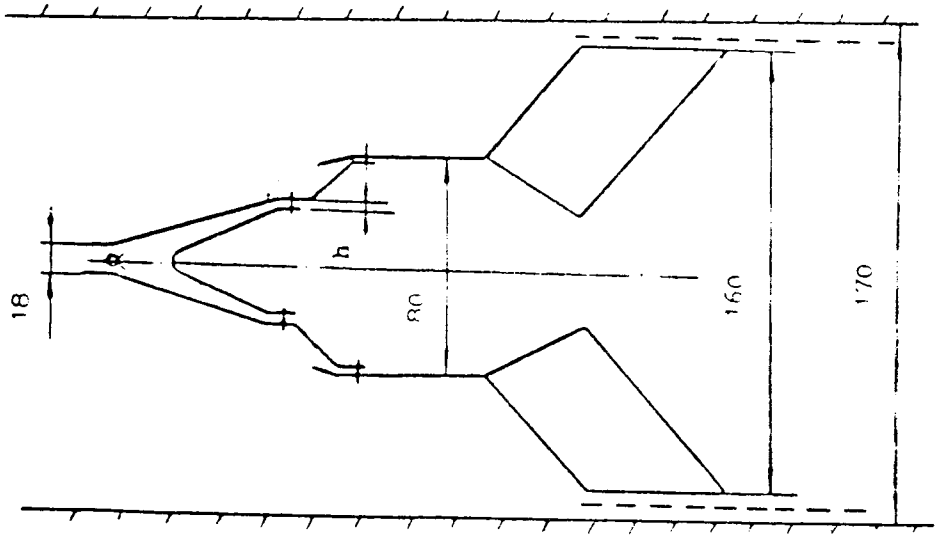

(b) Configuration SJ410-4B; h = 2, 3, 4, and 6 mm.

Figure 3. - Test configurations of piloted flameholders. (All dimensions in mm.)

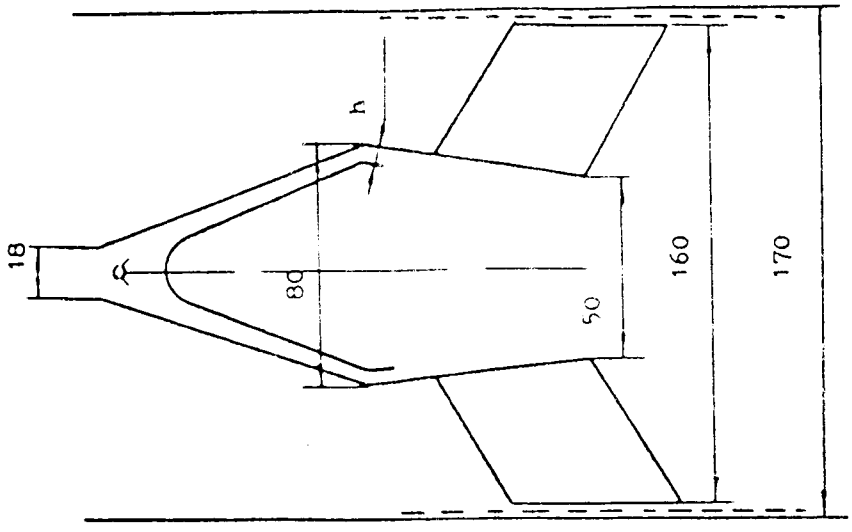

(c) Configuration SJ410-3A; h = 3, 5, and 7 mm.

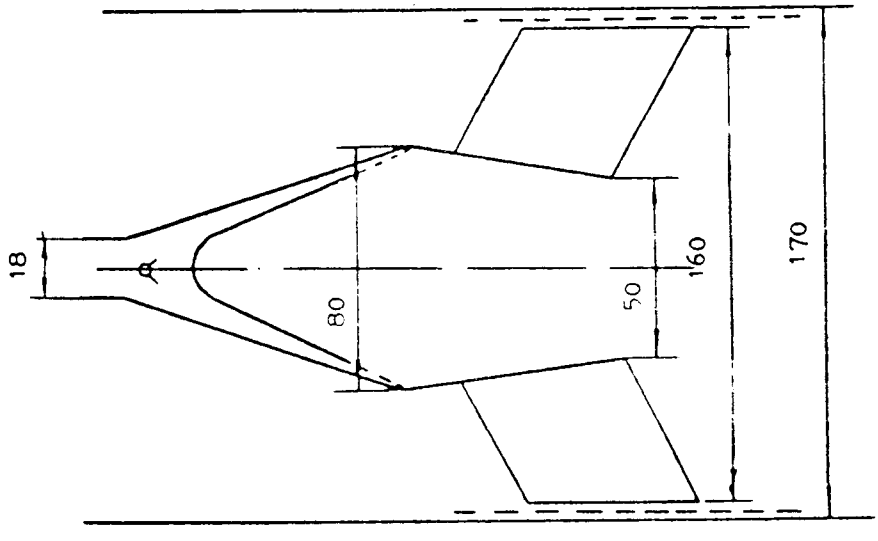

(d) Configuration SJ410-3B.

Type	Spacing	Number	Diameter
A	30	34	12mm
B	14	76	8mm
C	7	304	4mm

(e) Air-entry holes on the V-gutter.

Figure 3. - Concluded.

Type	A	B	C	D	E
P_2^* kg/cm^2	1.2	0.8	0.6	0.4	0.3
ΔP_2 kg/cm^2	0.057	0.047	0.051	0.0085	0.0085
$\Delta P_2/P_2^*$ %	4.8	5.9	2.5	2.1	2.8

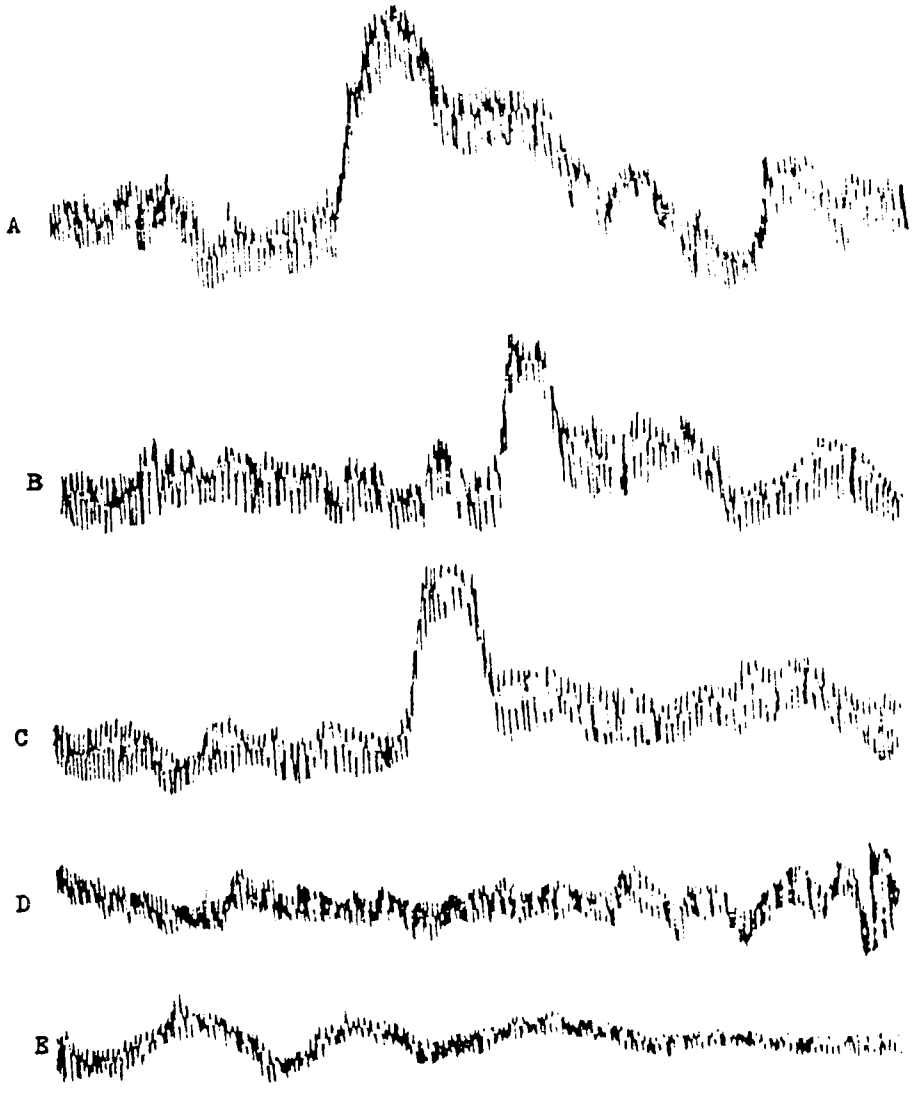

Figure 4. - Pressure oscillation during ignition.

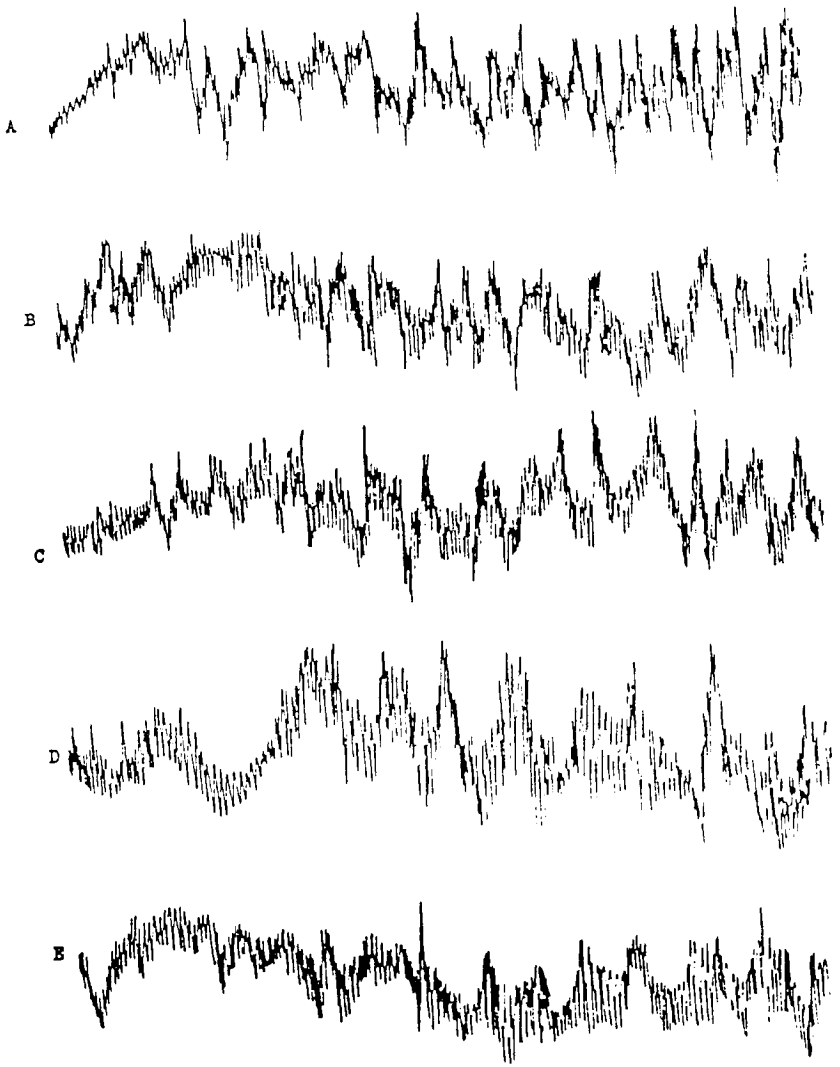

(a) Pressure oscillation during combustion starting in the secondary zone.

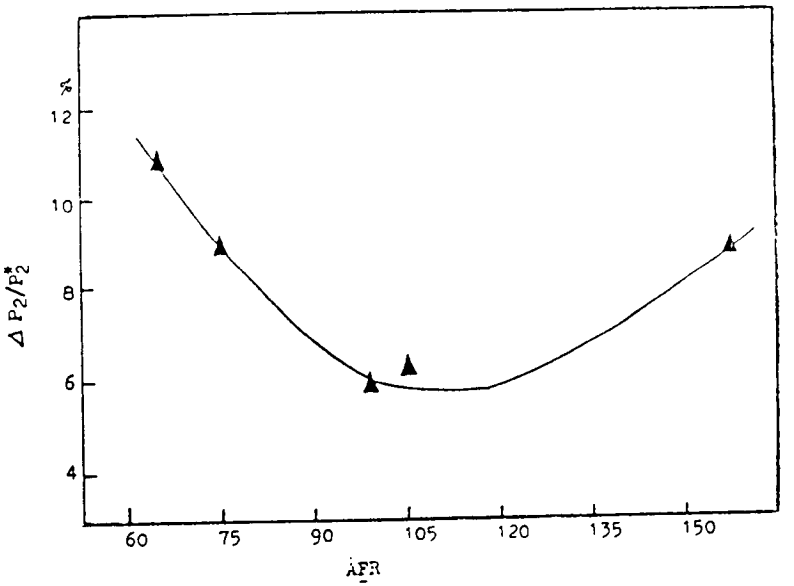

(b) Relation between the pressure oscillation and the fuel flow injected in the primary zone.

Type	A	B	C	D	E
P_2^* kg/cm^2	0.4	0.4	0.4	0.4	0.4
ΔP_2 kg/cm^2	0.034	0.024	0.036	0.043	0.025
$\Delta P_2/P_2^*$ %	8.5	6.0	9.0	11	6.3
AFR	157	100	74	65	104

(c) Test conditions.

Figure 5. - Pressure oscillation in the secondary zone.

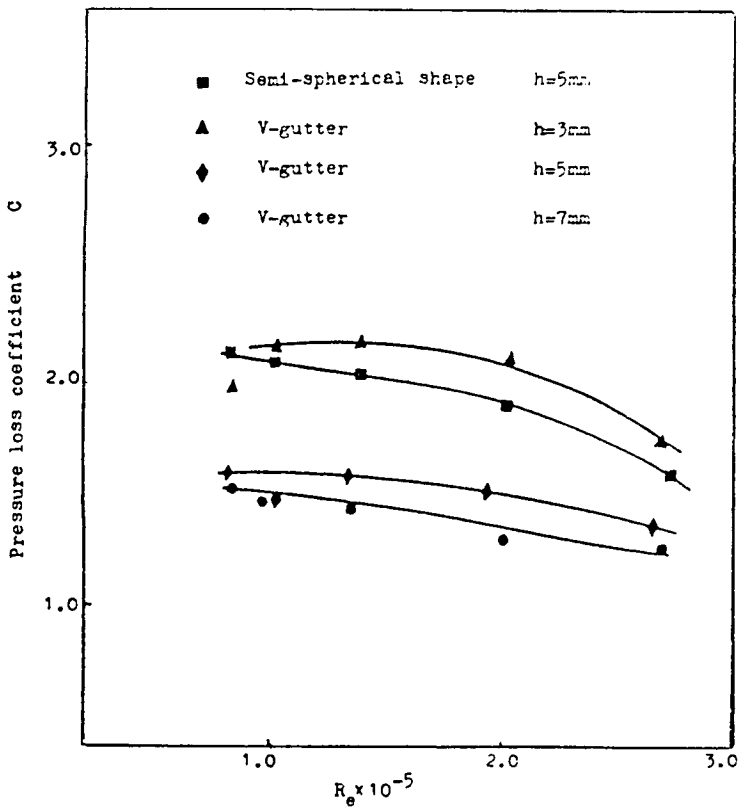

Figure 6. - Effect of shape and gap height on pressure loss coefficient.

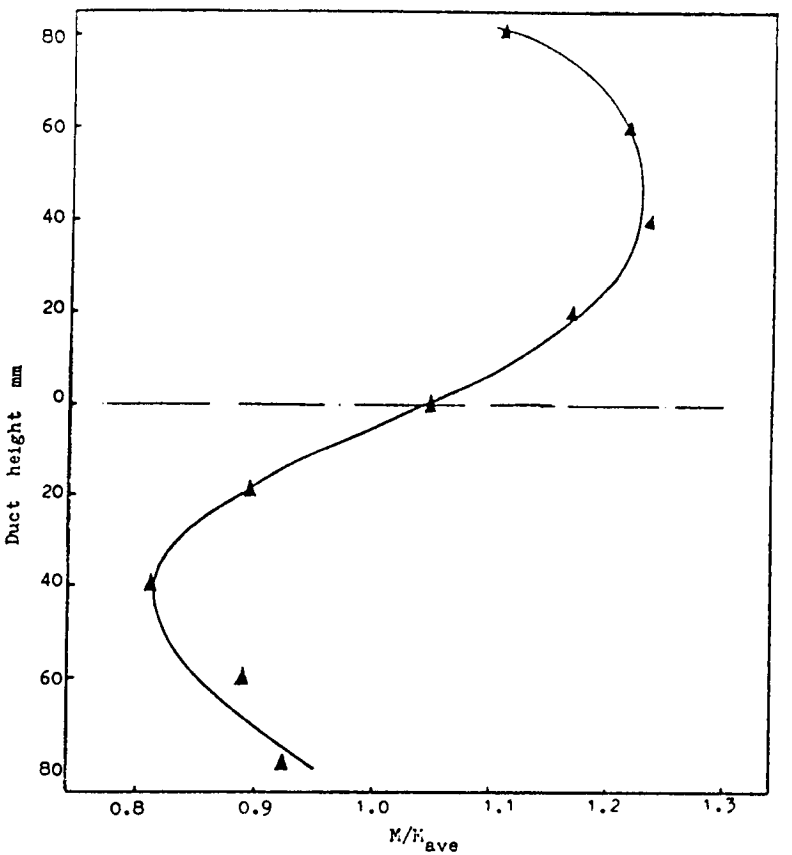

Figure 7. - Inlet flow distortion.

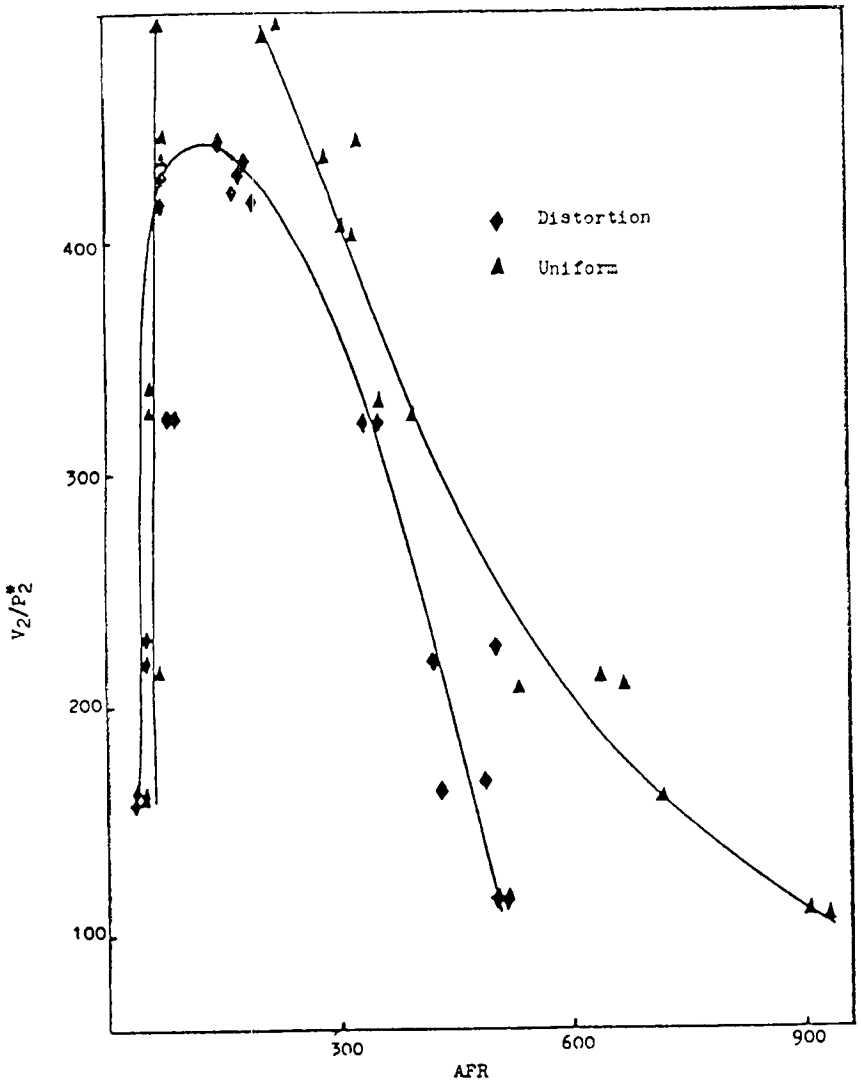

Figure 8. - Effect of inlet distortion on flame stabilization. Configuration SJ410-4B; T_2^* = 500 °C, M_2 = 0.23.

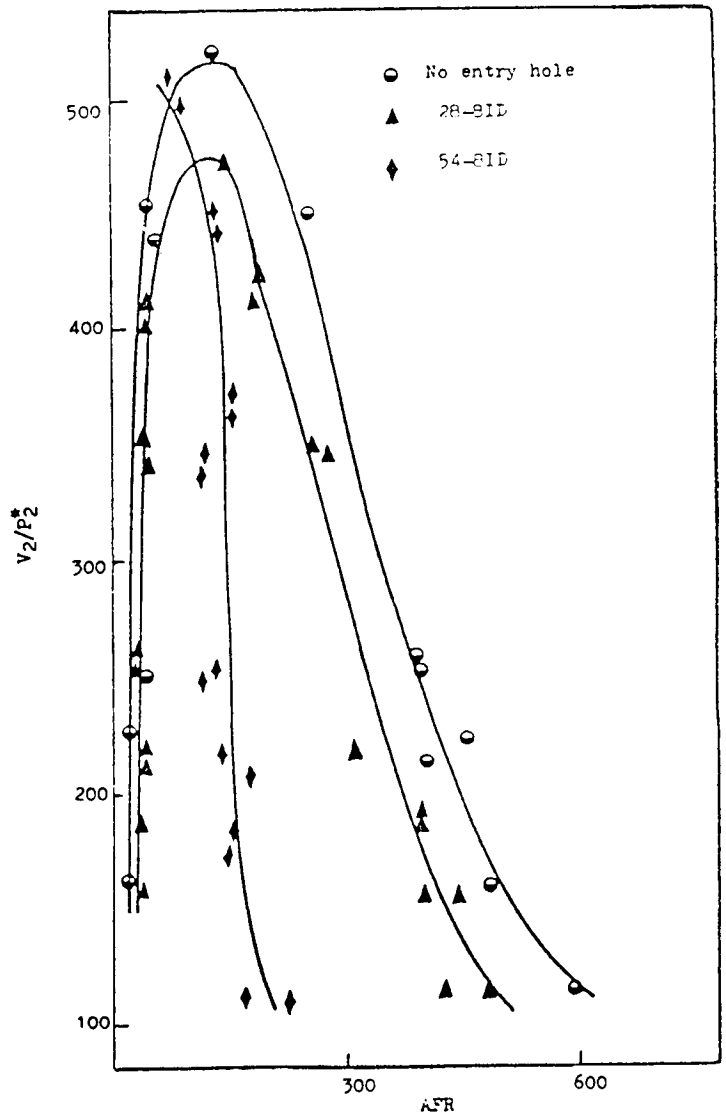

Figure 9. - Effect of secondary air-entry holes on flame stabilization. Configuration SJ410-4A; T_2^* = 500 °C, M_2 = 0.23.

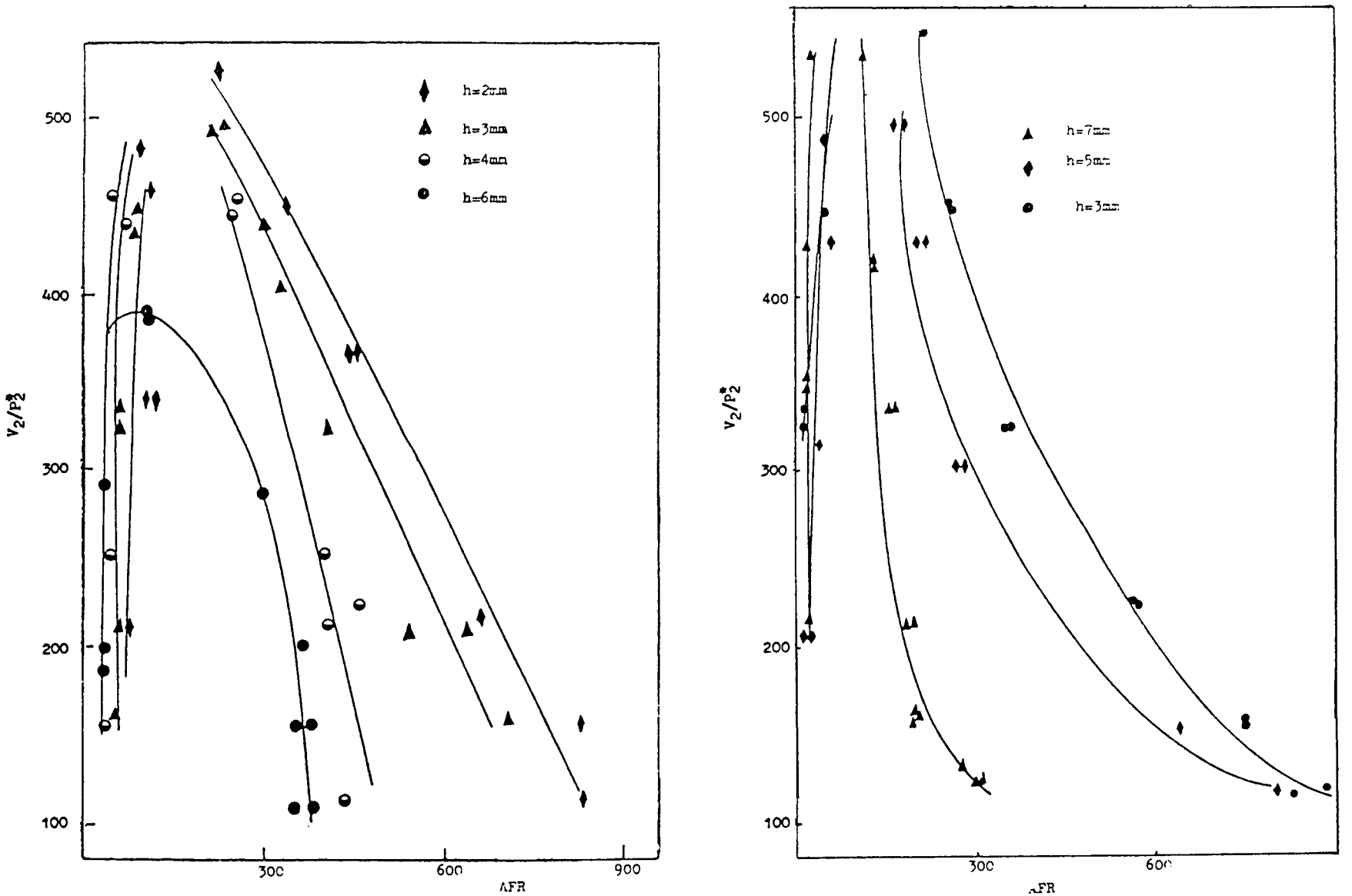

(a) Configuration SJ410-4B; T_2^* = 500 °C, M_2 = 0.23.

(b) Configuration SJ410-3A; T_2^* = 500 °C, M_2 = 0.23.

Figure 10. - Effect of gap height on flame stabilization.

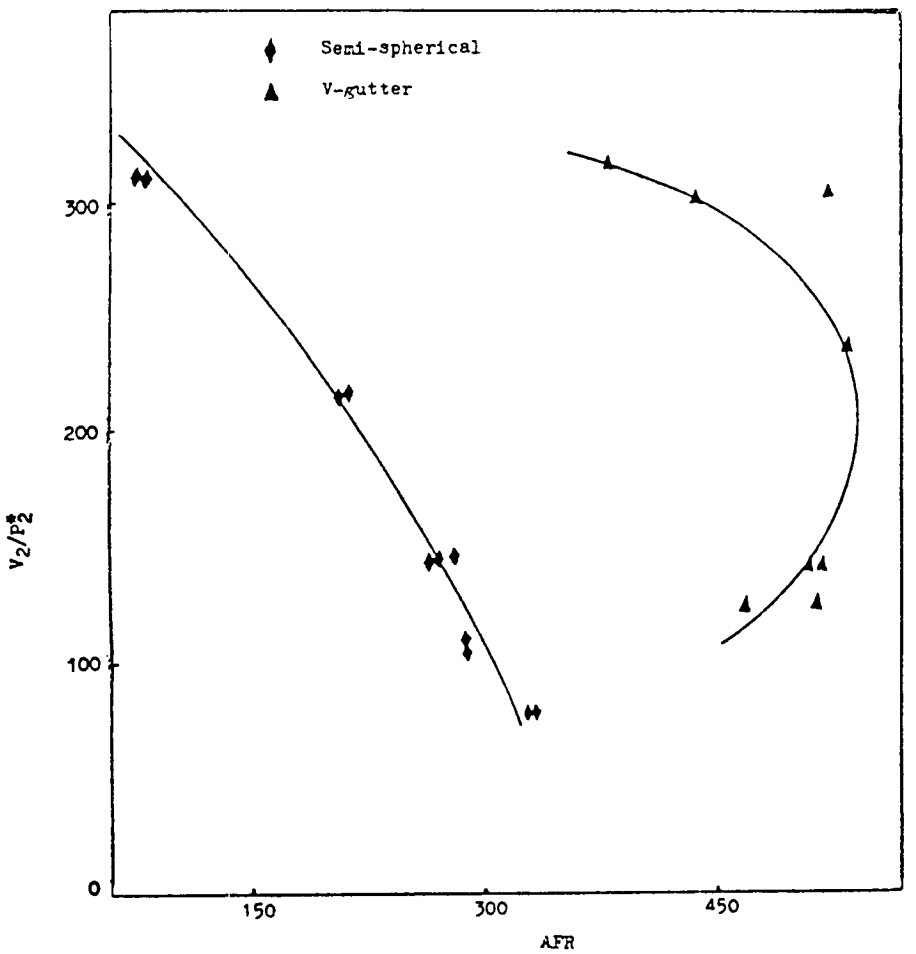

(a) Configuration SJ410-3A; T_2^* = 60 °C, M_2 = 0.23.

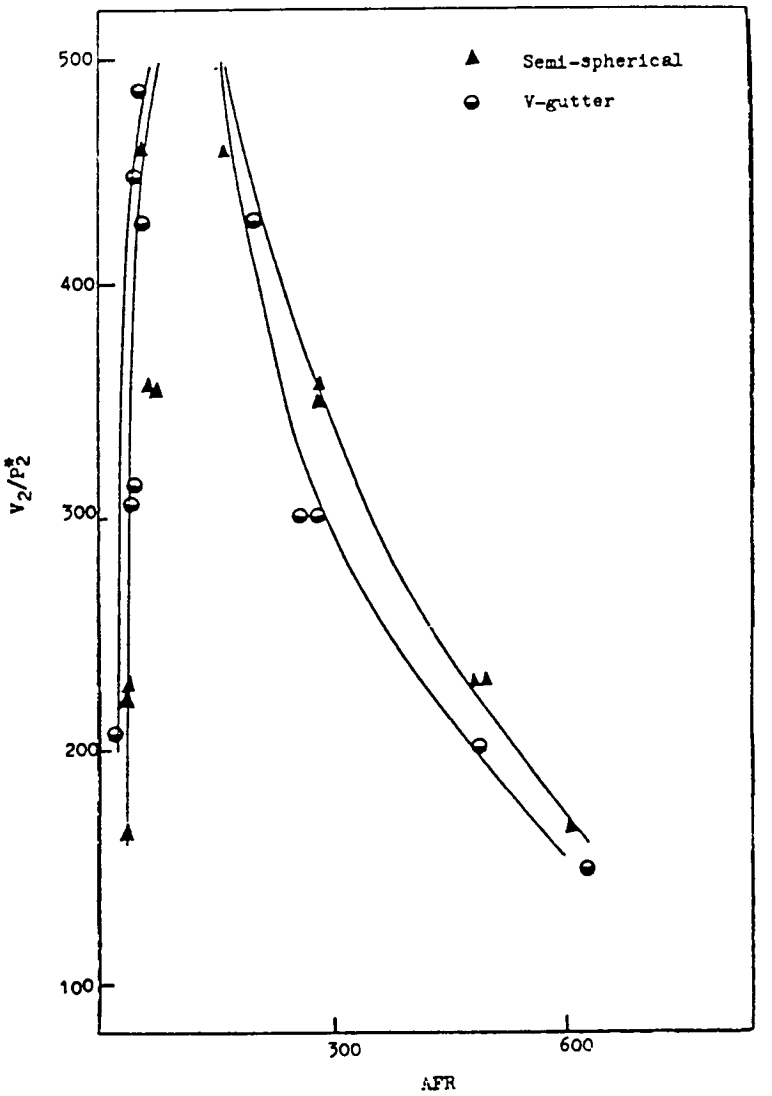

(b) Configuration SJ410-3A; T_2^* = 500 °C, M_2 = 0.23.

Figure 11. - Effect of bluff body shape on flame stabilization.

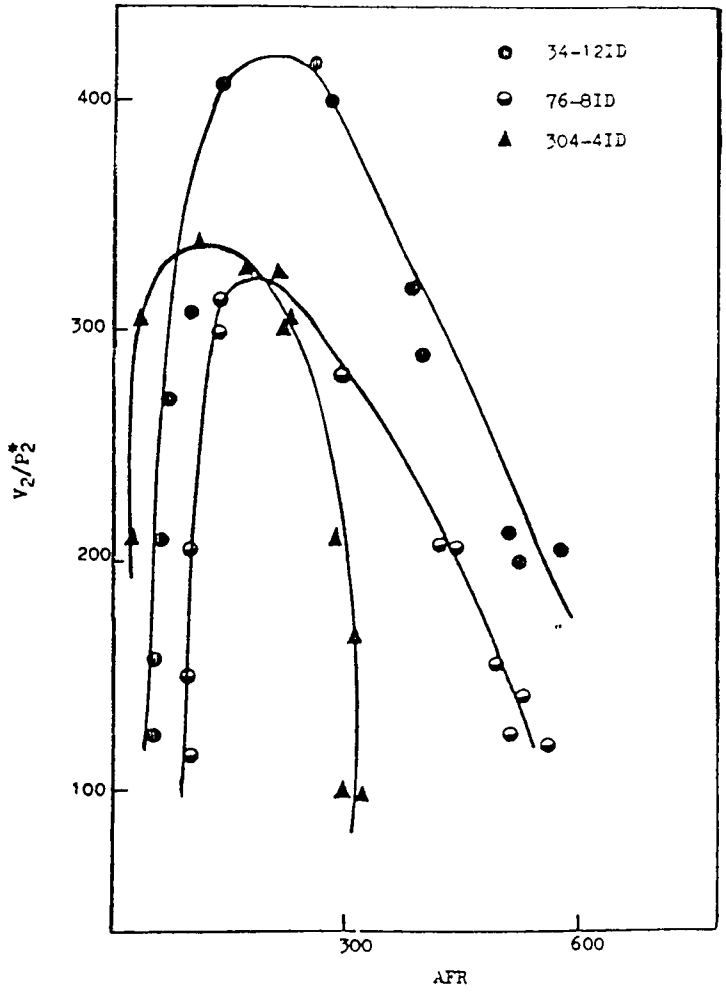

Figure 12. - Effect of air-entry holes in V-gutter wall on flame stabilzation. Configuration SJ410-3B; T_2^* = 500 °C, M_2 = 0.23.